Project title: Radiation risk appraisal for detrimental effects from medical exposure during management of patients with lymphoma or brain tumour (SINFONIA)

Grant Agreement: 945196

Call identifier: NFRP-2019-2020

Topic: NFRP-2019-2020-14 Improving low-dose radiation risk appraisal in medicine

Deliverable D3.2 - Methodology of an advanced computational approach and generation of new dose data for comforters in NUM

Lead partner:	SCK CEN (3)
Author(s):	Lara Struelens, Jérémie Dabin, Pasquale Lombardo
Work Package:	3
Delivery as per Annex I:	Month 24 (31.08.2022)
Actual delivery:	Month 24 (31.08.2022)
Type:	Report
Dissemination level:	Public

"This project has received funding from the Euratom research and training programme 2019-2020 under grant agreement No 945196"

Table of Contents

Abbreviations

^{99m}Tc	Technetium 99m
^{18}F	Fluor 18
^{131}I	Iodine 131
EANM	European Association of Nuclear Medicine
EMA	European Medicines Agency
EURADOS	European Radiation Dosimetry Group
Geant4	a toolkit for the simulation of the passage of particles through matter
GATE	advanced opensource software based on the geant4 toolkit
ICRP	International Commission on Radiological Protection

IPP	Interactive Posture Program
MCNP	Monte Carlo N-Particle Transport Code
NM	Nuclear Medicine
PHITS	Particle and Heavy Ion Transport code System
PODIUM	Personal Online Dosimetry using computational dosimetry
RAF	Realistic Anthropomorphic Flexible computational models

List of figures

List of tables

1. Introduction

The growing use of Nuclear Medicine (NM) and the diversity of new radiopharmaceuticals, stimulate the need for a more comprehensive re-evaluation of the radiological risk for caregivers and general public coming into proximity of NM patients. At present, these external doses are estimated by making a series of simplifications for modelling both the radiation emitted by the patient and the dose absorbed by the caregiver (or by a person from the general public). On the one hand, these approximations reduce the complexity of dose assessments, but on the other hand they also affect their accuracy. The objective of task 3.2 of SINFONIA is to develop a more comprehensive dose calculation approach by using the most recent advancements in computational dosimetry, such as Monte Carlo simulations, realistic human phantoms, and time activity distribution curves from the most recent biokinetic models.

1.1 Current situation: dosimetry limitations

In NM, patients are injected with radiopharmaceuticals for diagnostic and radiotherapeutic procedures. In order to ensure adequate radiation protection of the medical staff and the public, it is necessary to consider the impact of the radiation emitted by the patient, for example, when he/she is guided in the hospital or he/she leaves the hospital after the procedure. Such exposures may occur unknowingly to member of the public or knowingly to people who comfort the patients after the procedure, such as relatives.

Currently there is a limited number of studies on the assessment of potential external dose to caregivers and family. Most studies were performed for diagnostic procedures, where the patient is injected with ^{99m}Tc or ^{18}F. In case of therapeutic procedures, data can be found on ^{131}I therapy to treat thyroid cancer or hyperthyroidism. Although for the diagnostic applications, in general, studies indicate no need of any restrictions before a patient can be released from hospital, the issue is still in debate. For example, the EMA (European Medicines Agency) recommends avoiding close contact with children or pregnant women for 24h after injection in case of ^{99m}Tc procedures.

Existing guidelines are mainly related to ^{131}I therapy. In any case, most information available on the protection of caregivers of nuclear medicine patients, both for diagnostic and therapeutic procedures, is based on dose rate measurements in a single point at a certain distance from the patient and measured on several time points after injection. To assess the exposure level and possible risk to caregivers, these dose rate measurements are combined with assumed specific occupancy scenarios, describing how long caregivers are in close contact with the patient over time. Since the patient is a physically large radiation source, reducing that source to a dose rate in a single point is prone to lead to large errors in dose estimations, especially at short distances from that patient.

1.2 Objective of the project

In order to address current limitations, within task 3.2 a new dose calculation framework was developed where both the patient and the caregiver are explicitly modelled by using anthropomorphic computational phantoms, such as the ICRP 110 adult voxel phantoms. Among the library of phantoms, also new generation flexible phantoms were included. Thanks to these phantoms, the developed framework allows to generate models with arbitrary posture, position and rotation of both caregiver and patient bodies. Such flexibility makes it possible for our framework to model the actual geometrical setup of an exposure moment, which should benefit the accuracy of caregiver dose assessment. This flexibility is particularly important for modelling some of the most concerning close contact exposure situations, such as an adult holding/comforting a child patient, or a mother breastfeeding her child.

By stacking a series of exposure setups in a time sequence and by sampling the time activity curves of the relevant source organs for the radiopharmaceutical under study, this approach allows to generate dynamic exposure scenarios that can reproduce the actions typically performed by in- and out-patients, and caregivers, before and after release from the hospital. Building such types of dynamic scenarios and comparing the resulting doses, not only can support the creation of guidelines and recommendations for patient and caregivers, but it can also help to optimise hospital workflow, such as reducing or increasing the discharge time.

In this report, we present the developed software framework, its validation and 2 applications. In both validation and applications, external dose rates from nuclear medicine patients treated with ^{99m}Tc, ^{18}F and ^{131}I are evaluated. For validating the framework, the computational approach was benchmarked against experimental data in terms of ambient dose equivalent. As first application, we modelled a simplified scenario where an adult female patient is standing in front of an adult male caregiver. In the second application, an already more realistic exposure scenario is built by using the postural flexibility features of the framework.

2. Methodology

2.1 Layout of the computational dosimetry framework

Our computational framework is constituted by a series of workflows including sequences of both automated software and manual operations. The diagram in figure 1 summarizes the framework, with its workflows, and the steps that are executed to generate a caregiver exposure model.

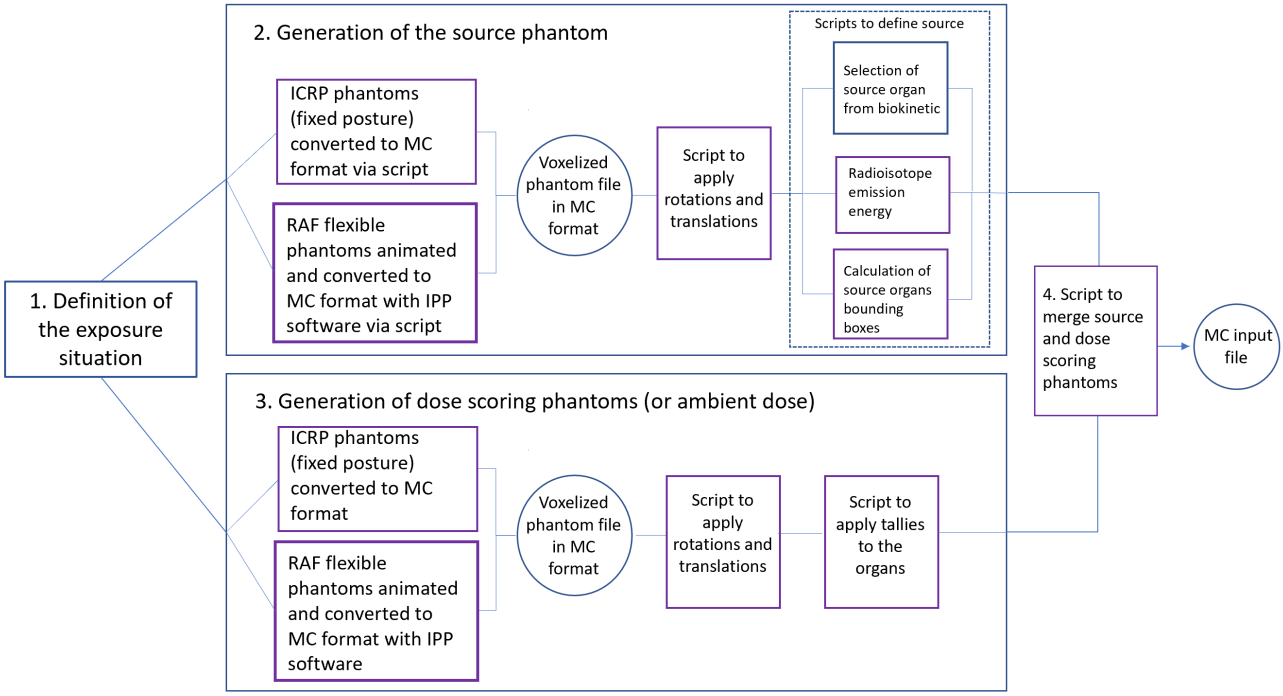

Figure 1. Diagram of the computational dosimetry framework, showing the workflows, the operations performed to generate a caregiver exposure model with two computational phantoms. Operations that are automated via software are represented with purple boxes, while operations requiring user input are represented with blue boxes. Files produced as output of operations are represented with circles.

Thanks to the available phantoms and geometries, the computational framework allows to generate 30 combinations of source-caregiver models by merging any of the 5 source phantoms with the 6 dose scoring methods (5 phantoms + ambient dose equivalent H*(10)), and any combinations with different postures and relative distances between the phantoms. The creation of the input files is largely automated, which allows to easily generate hundreds of simulations per day. This capability was made possible by developing application specific software to handle the complex geometry of the phantoms (especially the flexible ones), leaving only the simpler operations as manual input (for example, selecting the specific source organs based on the biokinetic of a radio-pharmaceutical).

In step 1, the exposure configuration is defined. With step 2, the source phantom is created by first selecting between the fixed ICRP reference phantoms and the flexible RAF phantoms. The phantoms are then converted into a voxelized format compatible with the chosen Monte Carlo (MC) code (MCNP, PHITS, GATE and Geant4 are supported). In the case of the ICRP, the conversion is performed via Python scripts, while in the case of the flexible RAF phantoms, the conversion is done automatically via the developed Interactive Posture Program (IPP). Based on the configuration defined in step 1, the voxelized patient phantom is translated and rotated in space. Finally, with the help of some scripts, the radioactive emission is added to the source organs as defined by the biokinetic model of each radio-pharmaceutical considered. In step 3, the dose scoring phantom representing the caregiver/member of the public/NM staff is created. For the large

part, the operations are similar to step 2; after creation of the voxel phantom, the caregiver model is translated and rotated according to the setup defined in step 1. However, in place of the scripts to attribute the source, in step 3 the organs are assigned dose scoring tallies. Finally, in step 4, the two phantoms representing source (patient) and dose scoring (caregiver) are merged in a single simulation file by means of a configurable script which can generate all desired combinations of phantoms.

In the section below we present the most relevant elements constituting this computational methodology.

2.1.1 Anthropomorphic computational models

The computational approach makes use of anthropomorphic models to represent both the patient and the caregiver. Within our dose calculation framework, five phantoms are available: the adult male and female voxel phantoms from ICRP Publication 110 [ICRP, 2009], and the house-made family of Realistic Anthropomorphic Flexible (RAF) polygonal mesh phantoms, including an adult male, an adult female and a 1-year-old female phantom (shown in figure 2).

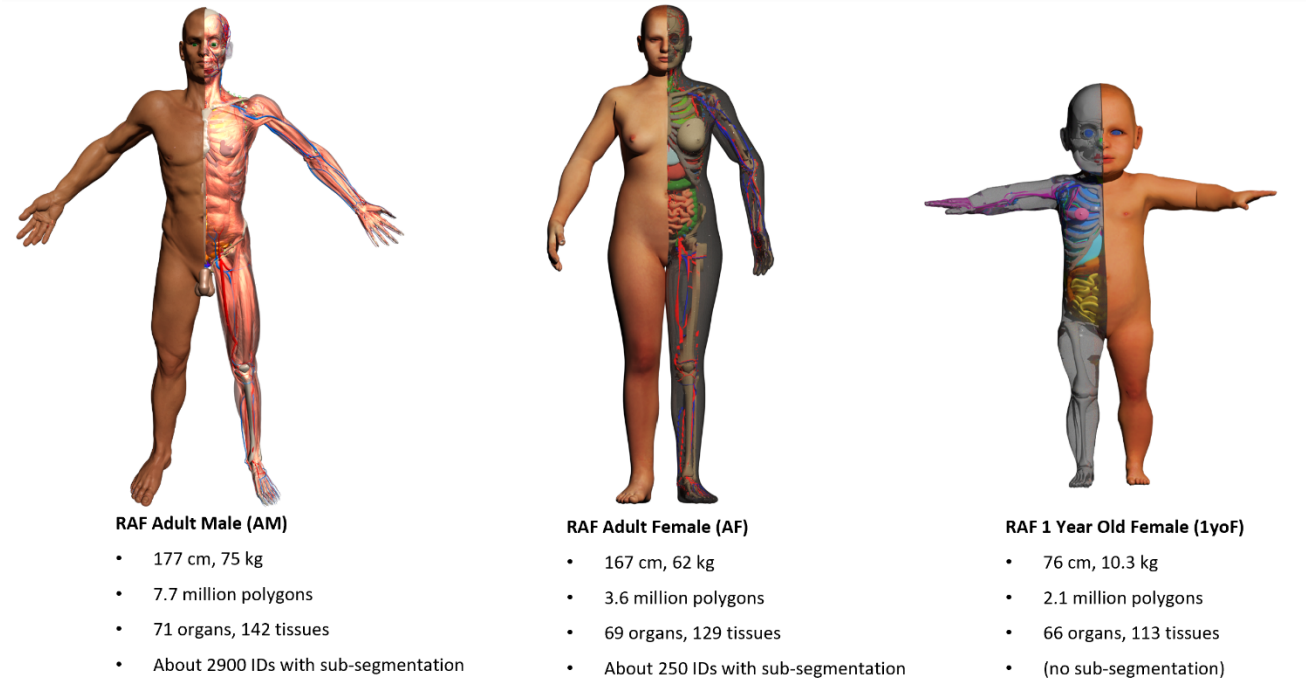

Figure 2. Cutaway view of the Adult Male (AM), Adult Female (AF), and 1 year old Female (1yoF) phantoms from the RAF phantoms family, and specifications of the mesh size, phantom dimensions, and number of tissues modelled. The sub-segmentation feature, available for the AM and AF phantoms, allows to further subdivide the tissues to facilitate the modelling of intra-organ activity distributions for the patient and/or to facilitate the scoring of intra-organ dose distributions of absorbed energy for the caregiver.

The ICRP voxel phantoms are considered the reference models for performing dose assessments in radiation protection. As they were created from segmentation of whole-body tomography, the ICRP phantoms anatomies are represented in voxel matrix format. While this format can be very detailed and anatomically accurate, it is also structured as a rigid lattice. This makes it difficult, if not impossible, to perform any modification of a voxel phantom. As a result, the postures of the ICRP phantoms are fixed to their original state, i.e., horizontally lying (on the tomography table). For this reason, they are used in our framework only for simulating vertically standing or horizontally lying patients and caregivers.

In the case of the RAF family, the phantoms were designed with a 3D graphic modelling software, 3Ds Max, by using the polygonal mesh format. Even if differences exist for some of the organs, the phantom anatomies have similar global dimensions to those of the reference ICRP phantoms. Also the materials and organ

densities of the RAF phantoms are analogous to the respective material and densities of the ICRP voxel phantoms [Lombardo, 2018]. The main difference lies in the high postural flexibility of the RAF phantoms, which results from the deformability of the polygonal mesh format, and that can be used to reproduce a more realistic patient/caregiver geometry. In fact, the high level of control over the posture of the RAF phantoms allows even to generate geometries for close contact exposure situations, such as that of an adult holding a child. However, the RAF phantoms polygonal mesh format is not yet compatible with Monte Carlo transport codes, requiring an intermediate conversion, known as voxelization, to enable the loading of flexible phantoms in Monte Carlo simulations. To change the phantom posture and to ease the creation of Monte Carlo simulation input files, the code of the in-house developed software named IPP (Interactive Posture Program) was modified including functions specific for modelling NM patients and caregivers. The IPP software was developed within the PODIUM project [Lombardo, 2019] to facilitate the use of flexible anthropomorphic phantoms, thanks to an interactive or scriptable graphic interface, and to automatically generate (including via batch scripting) Monte Carlo input files modelling interventional radiology environments, i.e., the main studied application of the PODIUM project.

Within SINFONIA, a modified version of IPP was developed with the purpose of generating models representing caregiver exposure. The first modification was the inclusion of the flexible Adult Female and the 1-year-old Female Child phantoms. Secondly, the interface of IPP was improved to allow a better control on the position and posture of the phantoms, in order to allow the creation of close contact situations. Figure 3 shows the graphic interface of IPP where the AM and the 1yoF phantoms were used to model a child patient being carried on the lap of her comforter. Finally, the support for exporting and converting the phantoms to additional Monte Carlo codes was added. So, besides MCNP (versions x, 5, 6), the software can convert the RAF phantoms to PHITS, Gate and Geant4 compatible formats.

Figure 3. Main graphical interface of the Interactive Posture Program (IPP).

2.1.2 Source organs and scoring of absorbed doses

Within the simulations, the organs of the patient phantom are defined as radioactive source organs, while the organs of the caregiver phantom are used to score energy depositions and, thus, absorbed doses. For the source modelling, the biokinetics of the radiopharmaceutical under study (^{99m}Tc, ^{18}F and ^{131}I) in the different source organs (i.e., how the radionuclide is distributed in the different source organs over time, see Table 1) are considered. The effect of each source organ to the caregiver dose is additive, which allows to optimize the number of simulations by defining just one organ as source per simulation. This allows to account for the biodistribution at a given moment post-injection by multiplying the dose effect of each source organ with the amount of activity at a certain time point. The total caregiver dose rate is then obtained by summing the dose contributes from all source organs for each time point.

Ionising radiation transport is simulated using a Monte Carlo radiation transport code to determine the external dose rates in proximity of the patient and to calculate the caregiver exposure, in terms of organ dose rates. Specifically, the scoring was performed using 3 dose metrics: ambient dose equivalent rate per MBq of injected activity (for comparing to measurements in the validation), organ and effective dose rates per MBq of injected activity in ICRP and flexible RAF phantoms.

Table 1. Radionuclide and source organ

Radionuclide	Source organs
^{99m}Tc	bladder, kidneys, bone and the remainder.
^{18}F	bladder, kidneys, liver, blood, brain, hearth, lungs, pancreas, spleen and the remainder
^{131}I	bladder, kidneys, liver, blood, salivary glands, stomach wall, thyroid, small intestine content, colon content and the remainder

2.2 Setup of the simulations

In order to have a gradual approach to the full complexity of flexible models representing close contact scenarios, the simulations were performed in 3 steps:

1. Validation of the computational approach by benchmarking against experimental data. In this step the dose rate in a point, in terms of ambient dose equivalent H*(10), is determined at a distance of 1m from the patient model.
2. Calculation of time-dependent absorbed dose rates in the organs of the caregivers' computational model, considering two computational models, one representing the patient and one representing the caregiver, both standing in front of each other at a distance of 1 m.
3. Calculation of time-dependent absorbed dose rates in the organs of the caregivers' computational model, considering a more complex close-contact scenario. This approach needs the use of deformable computational anthropomorphic models.

2.2.1 Validation of the computational approach

The first series of calculations are done with the nuclear medicine patient, represented by the ICRP female voxel phantom [ICRP, 2009]. The ambient dose equivalent *H*(10)* is determined by calculating the fluence in air in a point (represented as a small volume by a 1 mm^3 cube) at 1 m distance of the patient model at chest height. The set-up is illustrated in Figure 3a. Fluence is converted into H*(10) by using the energy-dependent conversion coefficients from ICRP-74 [ICRP, 1996].

The Monte Carlo simulations are performed with the radiation transport code PHITS versions 3.20 and 3.24 [Sato, 2018] for the 3 radioisotopes and GATE version 9.2 [Jan, 2004] only for ^{131}I. The simulation results are compared against:

- Simulation results obtained with three other Monte Carlo codes, performed within an EURADOS-EANM joint collaboration for the same geometry set-up. The following codes are included: *MCNPX* (performed at IRSN, France); *TRIPOLI-4* (performed at CEA France) [Brun, 2015]; *Geant-4* (performed at CHUV, Switzerland).
- Measurements of H*(10) at 1 m distance of nuclear medicine patients performed in seven different European nuclear medicine departments: University Hospital Centre Zagreb (for ^{99m}Tc), Lausanne University Hospital (for ^{99m}Tc), Charles University and University Hospital Motol (for ^{99m}Tc), Instituto Oncologico Veneto IRCCS (for ^{18}F), University Hospital Brussels (for ^{99m}Tc, ^{18}F), Hospital IsoPor-Azores, Portugal (for ^{131}I), Instituto de Medicina Nuclear, Portugal (for ^{99m}Tc, ^{18}F and ^{131}I)

The measurements are performed at different time points post-injection, with two measurements for each time point. An intercomparison exercise of the measurement equipment was performed. Dose rates were measured at one meter distance from a 99mTc vial with known activity. A coefficient of variation of 50% uncertainty was obtained. For the measurements, patient (sex and BMI) and procedure data (radiopharmaceutical, administered activity, residual activity after injection, number and timing of bladder voiding, if applicable) were collected.

In the second series of calculations, the caregiver is also represented by an ICRP voxel model (Figure 4b). Simulations are performed both with the male and the female ICRP voxel models. The effective dose to the caregiver is obtained as the average of the doses to the male and female models, weighed with ICRP 103 tissue weighting factors [ICRP 2007]. The nuclear medicine patient model and the caregiver model(s) are in straight position, facing each other with 1 m distance in between. Simulations are performed with PHITS and GATE (only for ^{131}I) and compared against the three Monte Carlo codes as mentioned above.

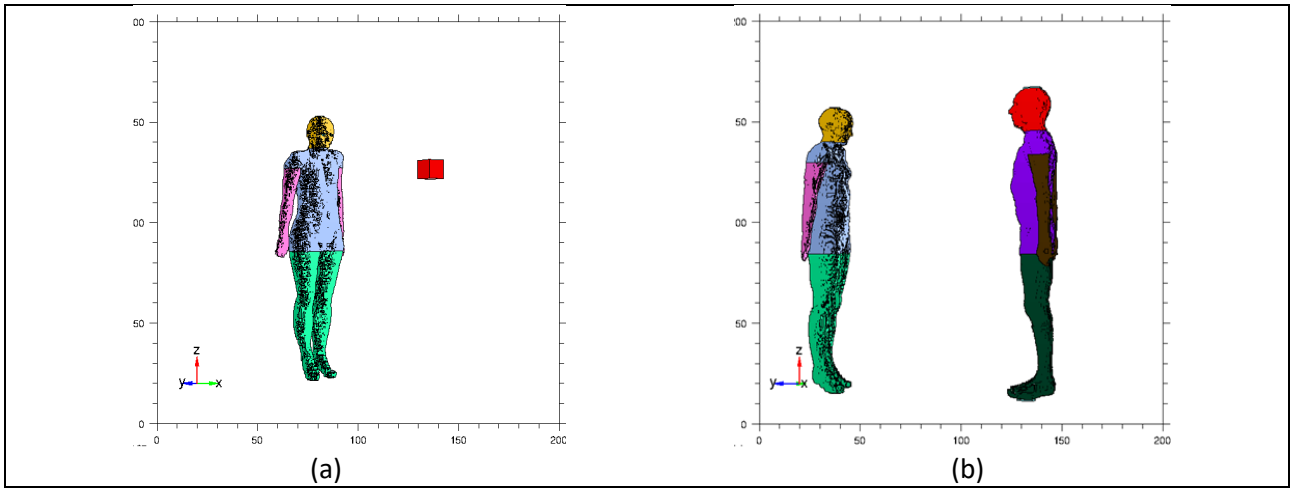

Figure 4. Monte Carlo geometry used to compare external dose rates at 1m distance from a nuclear medicine patient: dose rate in a point (a) and organ and effective dose rate in a caregiver model (b)

In the third series of calculations, the patient and caregiver models are represented by the male and female RAF polygonal mesh phantoms, which are developed at SCK CEN [Lombardo, 2018]. The simulations are performed with PHITS and compared against the PHITS simulations from the second series of simulations.

This benchmark study was performed for typical clinical procedures: ^{99m}Tc-HDP/MDP, ^{18}F-FDG, Na^{131}I. The biokinetic data for ^{99m}Tc and ^{131}I were taken from the ICRP-128 report [ICRP, 2015], which are considered suitable for the diagnostic ^{99m}Tc procedure and the treatment of hyperthyroidism with ^{131}I. The biokinetic data for ^{18}F-FDG were taken from the recently updated ICRP ^{18}F-FDG compartment model [Kamp, submitted to EJNMMI Physics; Andersson M, 2021].

The biokinetic models provide the relevant source organs for the respective radiopharmaceutical and how the amount of activity changes over time within each source organ. The simulations are performed for each source organ individually.

The cumulated H*(10) or effective dose rate per injected activity ([Sv/h]/Bq) is then calculated, for each time point (t) post-injection, as:

$$\frac{H^*(10)}{A_{inj}}(t) \; or \; \frac{E(t)}{A_{inj}} = \sum_{source\ organ} \left[A(t)_{source\ organ} * \frac{H^*(10) \; or \; E_{source\ organ}}{A_{inj}} \right]$$

with A(t) the fractional activity at time point (t) post injection in a specific source organ, $H^*(10)/A_{inj}$ and E/A_{inj}, the calculated ambient dose equivalent and effective dose, respectively, per simulated particle in a specific source organ.

2.2 Time-dependent absorbed organ dose rates for the caregiver in a close-contact scenario

For these simulations, the following close-contact scenarios are considered, considering ^{131}I treatment for hyperthyroidism:

- A female nuclear medicine patient sleeping in the same bed as a male family member, at a distance of 50 cm (Figure 6a). This is the same configuration as the two computational models standing straight in front of each other, but at a smaller distance.
- A female nuclear medicine patient in sitting position at 30 cm next to a sitting family member (representing a close-contact scenario at home) or next to a sitting member of the public, (representing close contact by using public transport) (Figure 6b)

The deformation of the polygonal mesh RAF phantoms, according to the considered scenarios is done with the IPP software (Interactive Posture Program), developed at SCK CEN. Before implementation in the Monte Carlo code, the mesh phantoms are voxelised and used to calculate the time-dependent organ dose rates per injected activity to the caregiver, considering the ^{131}I biokinetics in the patient model from the ICRP-128 report [ICRP, 2015].

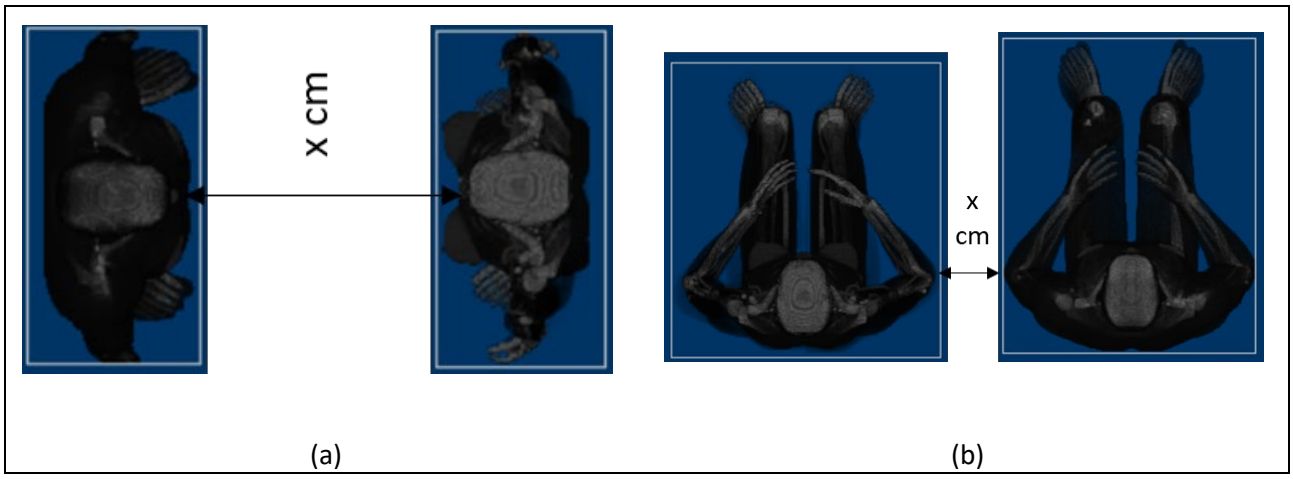

Figure 5. The Monte Carlo geometry used to simulate specific close-contact scenarios with a female nuclear medicine patient: straight position at 50 cm distance (a) sitting position at 30 cm distance (b).

3. Results

3.1 Validation of the computational approach

3.1.1 ^{99m}Tc-HDP/MDP

In Figure 6, $H^*(10)$ dose rate per injected activity in a point at 1 m distance from the patient model is shown for the four Monte Carlo codes. The statistical uncertainty on the simulations for each code is smaller than 5%. The variation between the different MC codes ranges from 5% to 10% for the different source organs. The fast drop in H*(10) at 210 min post injection, corresponds to the standard bladder voiding time, implemented in the ICRP biokinetic model.

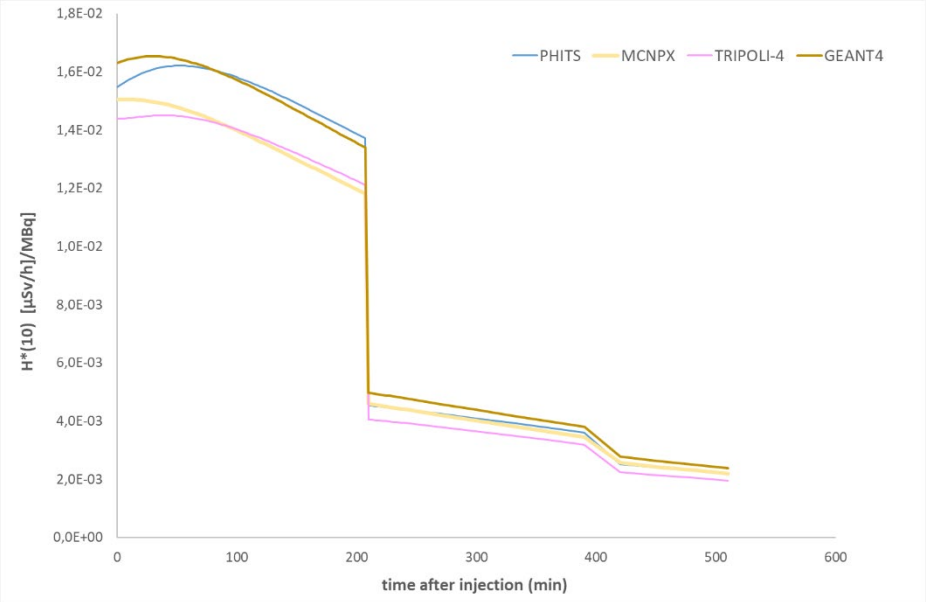

Figure 6. H*(10) dose rates per injected activity over time post-injection for ^{99m}Tc in a point at 1m distance from the patient at chest level for four different Monte Carlo codes.

From the measurement data, it was observed that the bladder voiding by the patient is requested prior to the SPECT scan, which is usually scheduled on average 120 min post injection (interquartile range: Q1=91 min - Q3=157 min; min=27 min; max=234 min). Therefore, for comparison to the measurements, the biokinetic model for the urinary bladder from ICRP-128 has been adjusted to more realistic bladder voiding times. The experimental data was categorised according to the first bladder voiding time for each patient and compared against the simulated data combined with the biokinetic model with a similar bladder voiding regime (Figure 7). In that case, a good agreement was found between the simulations and the measurements.

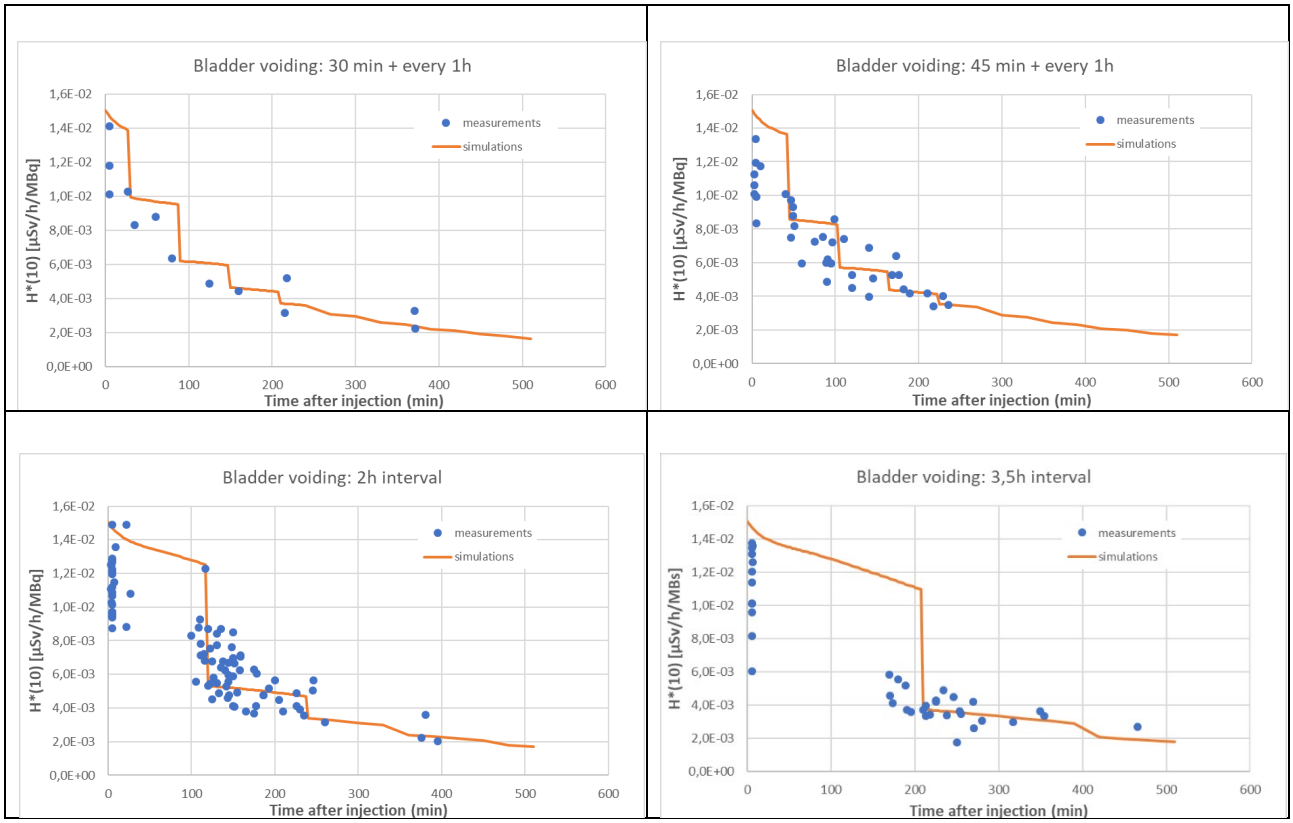

Figure 7. Comparison of simulation data and experimental data for H*(10) dose rate determination at 1m distance of nuclear medicine patients, according to first bladder voiding time

In Figure 8, simulations are compared between the different Monte Carlo codes when the effective dose rate per injected activity is calculated over time post-injection, with both the nuclear medicine patient and the caregiver represented by the ICRP reference computational voxel phantoms. The variation between the codes was lower than 8% for the different source organs. A thorough comparison of the simulation parameters and geometry implementation within the codes, showed that the variation comes mainly from geometrical differences in terms of the actual distance between the two phantoms. The distance between both phantoms is smallest for the MCNP-X and TRIPOLI-4 codes, with 2 to 4 cm closer compared against the implementation of the models within PHITS and Geant-4, explaining the higher resulting dose values.

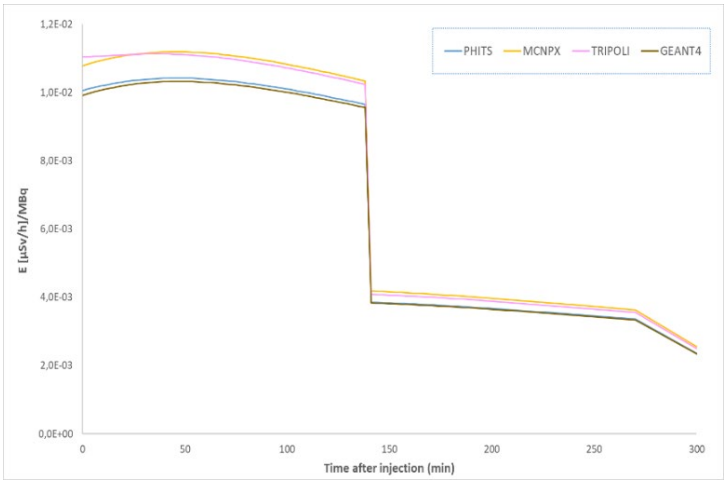

Figure 8. Effective dose rates per injected activity over time post-injection for ^{99m}Tc for a computational model at 1m distance from the patient model, comparing four Monte Carlo codes.

3.1.2 ^{18}F-FDG

In Figure 9, $H^*(10)$ dose rate per injected activity in a point at 1 m distance from the patient model is shown, for the four Monte Carlo codes. The statistical uncertainty on the simulations for each code is smaller than 5%. The variation between the codes is less than 4% for the different source organs. The measurement data from three hospitals is also included, which confirmed a bladder voiding time on average around 1h post-injection. The ICRP ^{18}F-FDG compartment model was adjusted accordingly for the urinary bladder. Good agreement is observed between experimental and simulation data.

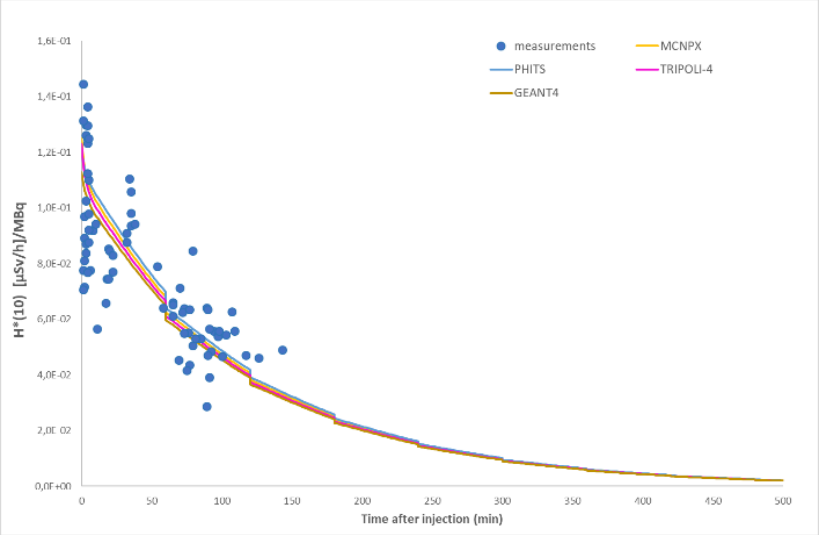

Figure 9. Comparison of simulation data and experimental data for H*(10) dose rate determination at 1m distance of nuclear medicine patients, injected with ^{18}F

In Figure 10, simulations are compared between the different Monte Carlo codes when the effective dose rate per injected activity is calculated over time post-injection, with both the nuclear medicine patient and the caregiver represented by the ICRP reference computational voxel phantoms. The variation between the codes was lower than 7% for the different source organs.

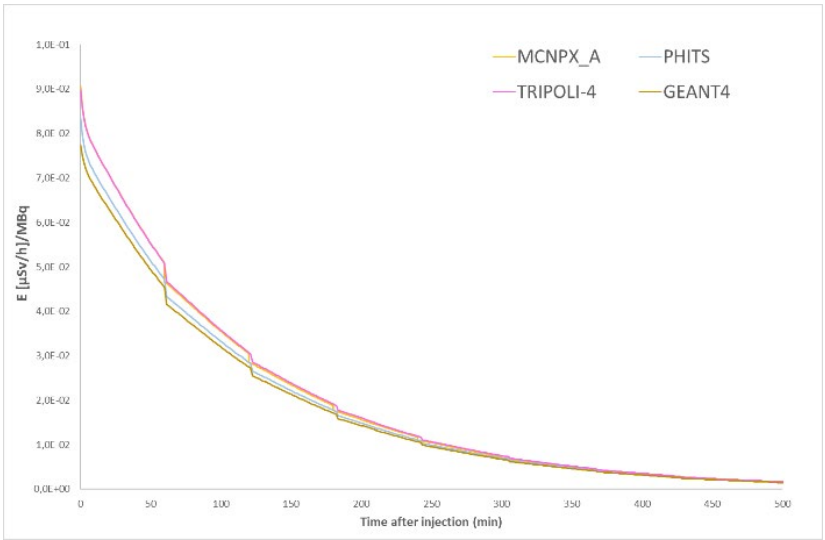

Figure 10. Effective dose rates per injected activity over time post-injection for ^{18}F for a computational model at 1m distance from the patient model, comparing four Monte Carlo codes.

3.1.3 $Na^{131}I$

In Figure 11, $H^*(10)$ dose rate per injected activity in a point at 1 m distance from the patient model is shown, comparing five Monte Carlo codes for ^{131}I. The variation between the different codes is less than 5% for the different source organs. The measurement data from one hospital is included. Measurements are performed with patients treated for hyperthyroidism. As there are non-hospitalised patients, only early time points are available. Again, good agreement is observed between experimental and simulation data.

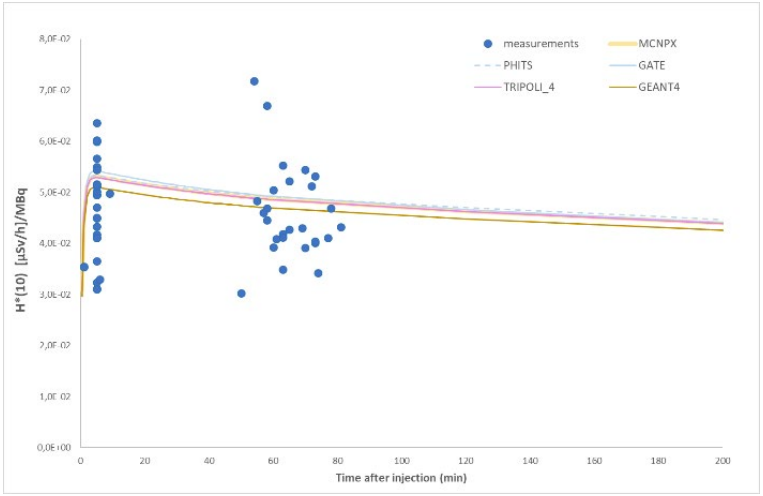

Figure 11. Comparison of simulation data and experimental data for H*(10) dose rate determination at 1 m distance of nuclear medicine patients, administered with ^{131}I

In Figure 12, simulations are compared between five Monte Carlo codes when the effective dose rate per injected activity is calculated over time post-administration, with both the nuclear medicine patient and the caregiver represented by the ICRP reference computational voxel phantoms. The variation between the codes was lower than 8% for the different source organs.

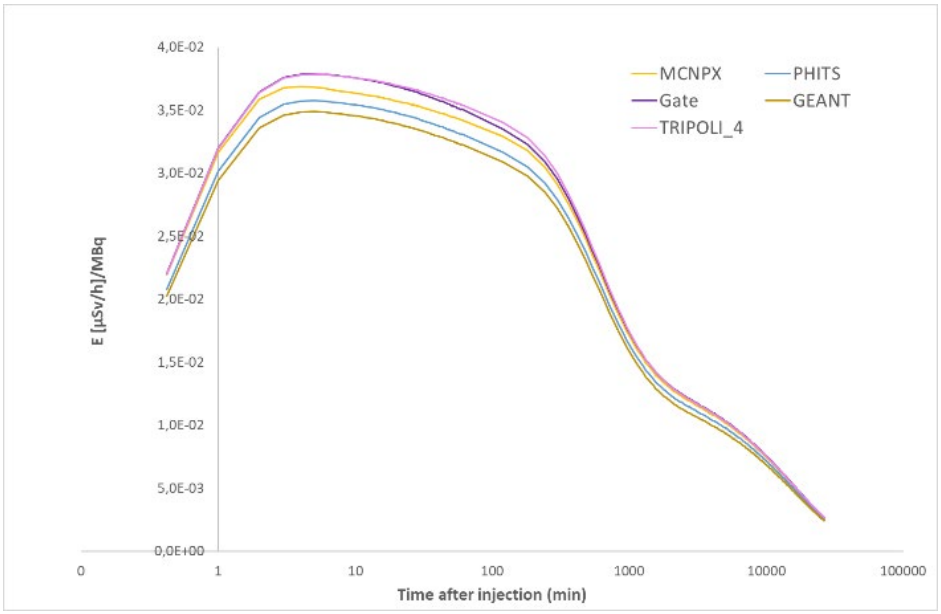

Figure 12. Effective dose rates per administered activity over time post-injection for ^{131}I for a computational model at 1m distance from the patient model, comparing five Monte Carlo codes.

In Figure 13, simulations with PHITS are compared when the effective dose rate per injected activity is calculated on one hand using the ICRP reference computational voxel phantoms and on the other hand, using the RAF polygonal mesh phantoms for both patient and caregiver models at 1 m distance from each other. The effective dose rate per injected activity is on average 14% lower (range: 6% - 43% over the different source organs) when using the flexible polygonal mesh phantoms. An important contribution here is the voxelisation step for the polygonal mesh phantoms, that can have an impact of up to 10% on the sizes and masses of the different organs, both for the patient and the caregiver model. Both phantom models are obviously not completely anatomically identical, which is also not the case for a patient population. The observed difference is acceptable for the purpose of this study, considering other types of uncertainties, such as the choice of biokinetic model and the fact that a patient and caregiver can differ a lot in size from any chosen computational model.

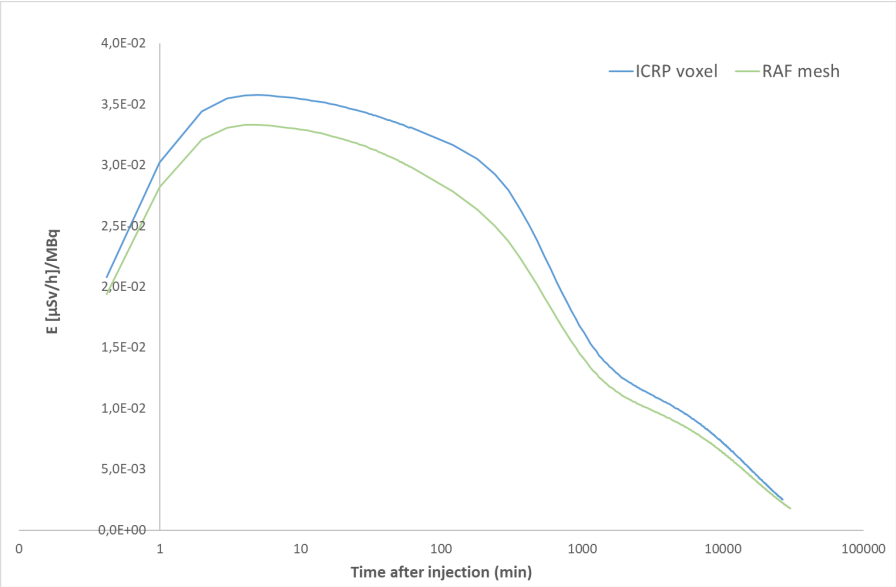

Figure 13. Effective dose rates per administered activity over time post-injection for ^{131}I comparing 2 types of computational models at 1m distance.

3.2 Time-dependent absorbed organ dose rates for the caregiver in a close-contact scenario

In figure 14, the absorbed dose rates are shown for two possible close-contact scenarios for a nuclear medicine patient administered with ^{131}I:

- The female RAF (as nuclear medicine patient) at 50 cm distance from the male RAF phantom, representing scenarios such as partners sleeping in the same bed, or any home-situation where partners are not keeping any distance. In this case the posture of the polygonal mesh phantoms is unchanged.
- The female RAF (as nuclear medicine patient) in sitting position, next to the male RAF phantom, also in sitting position, 30 cm from each other.

For comparison, the *H*(10)* dose rate at 1 m from the nuclear medicine patient is included, as this is the current approach used nowadays to assess the exposure to caregivers from these patients.

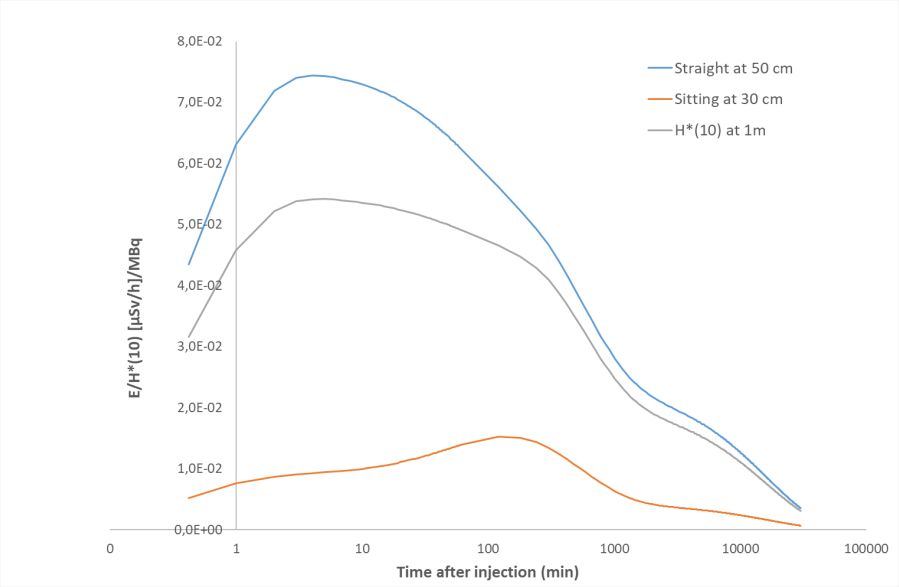

Figure 14. Effective dose rates per administered activity over time post-injection for ^{131}I for two more realistic close-contact scenarios, and comparting against the H*(10) approach in a point at 1 m distance for the patient.

It is clear that the dose rate from a nuclear medicine patient, with also the caregiver in sitting position results in lower external exposure, compared to when both models are in standing position, even for a very small distance between both models. The configuration where the two models are in straight standing position result in external dose rates that are following the same trend as for the H*(10) in a point approach, only the distance is the major impact parameter.

4. Conclusion and discussion

This first report demonstrates that the computational framework that has been developed to assess the external dose rate from nuclear medicine patients and the resulting exposure to caregivers, nuclear medicine staff or the general public is well validated.

The validation has been performed successfully on one hand against experimental data of H*(10) at 1 m distance from a nuclear medicine patient. Next, several Monte Carlo codes agreed well in a more complex scenario where both the nuclear medicine patient and the caregiver are represented by anthropomorphic computational models. The largest uncertainty in modelling the external dose rates of nuclear medicine patients come from the choice or availability of biokinetic model for the isotope under study. The available models from ICRP are developed for healthy people, while the biokinetics from patients with a specific disease can vary significantly. Recently, efforts were done [Taprogge, 2021] or ongoing to update these ICRP models, with available patient data to obtain biokinetic information which is more representative for nuclear medicine patients. The results from the computational framework can easily be updated with new and more appropriate biokinetic information.

The simulation framework comes with a variety of uncertainties. In table 2, an overview of the different uncertainty sources in the simulated dose rates is given. The statistical uncertainty of the Monte Carlo simulations itself was systematically not higher than 5% and in most cases even smaller than 1%. A sensitivity study investigated the effect of performing the simulations with a simplified spectrum (i.e. only photons contributing more than 1% to the total number of photons per disintegration) against the complete energy spectrum. The differences were never higher than 6%. Another uncertainty is the implementation of the distance between the 2 computational models, when defining the distance from skin to skin of both models. Another sensitivity study (performed in the framework of EURADOS collaborations) showed differences between the different code users up to 10 cm for the predefined distance of 1m between both phantoms. This resulted in differences in dose rate calculations less than 15% for ^{99m}Tc and less than 10% for ^{18}F and ^{131}I. The largest uncertainty in modelling the external dose rates of nuclear medicine patients come from the choice or availability of biokinetic model for the isotope under study. The available models from ICRP are developed for healthy people, while the biokinetics from patients with a specific disease can vary significantly. Recently, efforts were done [Taprogge, 2021] or ongoing to update these ICRP models, with available patient data to obtain biokinetic information which is more representative for nuclear medicine patients. Currently, the associated uncertainty cannot be quantified, but as the computational framework can easily be updated with new and more appropriate biokinetic information, the effect of choosing different models can be investigated. There is also the uncertainty related to the choice of computational models to represent both the patient and the caregiver. Real patients and caregivers will never be an exact copy of these models. A sensitivity study will be performed in the frame of the EURADOS collaboration to determine the effect of the phantom anatomy. Normalised dose rates will be simulated for different phantom body shapes. This can be easily implemented with the IPP software in combination with the RAF phantoms.

Table 2. Uncertainty sources in the simulated dose rates

Uncertainty source	**Value (%)**
Statistical uncertainty	<5%; mostly <1%
Simulated energy spectrum	<=6%
Distance between computational models (up to 10cm variation)	Tc-99m: <15% I-131:<10% F-18<10%
Phantom-patient anatomy	Not quantified*
Biokinetic model	Not quantified*

**Sensitivity study to be performed*

Finally, the use of polygonal mesh phantoms has been compared against the ICRP reference voxel phantoms for one specific isotope (^{131}I) and one Monte Carlo code (PHITS). This final benchmark was important as for the next part of the study, close-contact scenarios will be simulated, using these polygonal mesh phantoms, which are flexible and therefore can be used for a large variety of postures and combinations between patient and caregiver/staff/public member. As a first demonstration, the phantoms have been used in some relatively easy configurations, like standing up at close distances or in a sitting position. In the follow-up of the study, more scenarios will be modelled, focussing on more critical scenarios as mother-child combinations. In this case, the child can be as well the nuclear medicine patient, exposing the mother (which could be pregnant or not); or the child might also be exposed by the mother, when she is the nuclear medicine patient.

The IPP software was developed to ease the replicability and reproducibility of the whole computational approach, so that the framework can be applied to simulate hundreds, potentially thousands of exposure configurations by varying phantoms, bodies position, posture, radionuclide emission, etc… In this way, this approach will be helpful for assessing caregiver doses also in the future, when new radiopharmaceuticals will be adopted for treatment and diagnosis in NM.

The expected outcome on the longer term from such a more advanced computational framework is a database of effective dose rates per injected activity for a large variety of close-contact configurations, for a range of isotopes and radiopharmaceuticals. Hospitals or authorities can use such a database to evaluate the exposure to caregivers or the general public for specific scenarios, compare them against specific constraints of interest and develop guidelines for the nuclear medicine patient. Moreover, besides determining the effective dose rate, also organ-specific dose rates per injected activity, such as gonad dose rates, eye lens dose rates or foetus dose rates can be calculated separately.

References

Andersson, 2021: A revised compartmental model for biokinetics and dosimetry of 18F-FDG. M. Andersson, A. Kamp, D. Noβke, S. Mattsson, A. Giussani, Oral presentation at EANM 2021

Brun E., F. Damian, C.M. Diop, E. Dumonteil, F.X. Hugot, C. Jouanne, Y.K. Lee, F. Malvagi, A. Mazzolo, O. Petit, J.C. Trama, T. Visonneau, A. Zoia, Tripoli-4®, CEA, EDF and AREVA reference Monte Carlo code, Annals of Nuclear Energy 82, 151-160 (2015).

ICRP, 1996: Conversion Coefficients for use in Radiological Protection against External Radiation. ICRP Publication 74. Ann. ICRP 26 (3-4).

ICRP, 2007. The 2007 Recommendations of the International Commission on Radiological Protection. ICRP Publication 103. Ann. ICRP 37 (2-4).

ICRP, 2009: ICRP, 2009. Adult Reference Computational Phantoms. ICRP Publication 110. Ann. ICRP 39 (2).

ICRP, 2015: Radiation Dose to Patients from Radiopharmaceuticals: A Compendium of Current Information Related to Frequently Used Substances. ICRP Publication 128. Ann. ICRP 44(2S)

Jan, 2004: GATE: a simulation toolkit for PET and SPECT. S Jan , G Santin, D Strul, S Staelens, K Assié, D Autret, S Avner, R Barbier, M Bardiès, P M Bloomfield, D Brasse, V Breton, P Bruyndonckx, I Buvat, A F Chatziioannou, Y Choi, Y H Chung, C Comtat, D Donnarieix, L Ferrer, S J Glick, C J Groiselle, D Guez, P F Honore, S Kerhoas-Cavata, A S Kirov, V Kohli, M Koole, M Krieguer, D J van der Laan, F Lamare, G Largeron, C Lartizien, D Lazaro, M C Maas, L Maigne, F Mayet, F Melot, C Merheb, E Pennacchio, J Perez, U Pietrzyk, F R Rannou, M Rey, D R Schaart, C R Schmidtlein, L Simon, T Y Song, J M Vieira, D Visvikis, R Van de Walle, E Wieërs, C Morel. Physics in Medicine and Biology 2004 Vol. 49 Issue 19 Pages 4543

Kamp, 2022: A revised compartmental model for biokinetics and dosimetry of 18F-FDG, submitted to EJNMMI Physics

Lombardo, 2018: Development and Validation of the Realistic Anthropomorphic Flexible (RAF) Phantom. Lombardo, Pasquale; Vanhavere, Filip; Lebacq, Anne Laure; Struelens, Lara. In: Health physics, Vol. 114, No. 5, 02.05.2018, p. 486-499.

Lombardo, 2019: D9.104 - Database of phantoms of different statures and postures. Lombardo Pasquale, M. Zankl. Deliverable of the PODIUM EC founded project. Full text available at: https://concert-h2020.eu/sites/concert_h2020/files/uploads/Deliverables/D9/Podium/_Lists_Deliverables_Attachments_88_D9.104_Database-of-Phantoms_approved08112018.pdf

Sato 2018: Features of Particle and Heavy Ion Transport code System (PHITS) version 3.02. Tatsuhiko Sato, Yosuke Iwamoto, Shintaro Hashimoto, Tatsuhiko Ogawa, Takuya Furuta, Shin-ichiro Abe, Takeshi Kai, Pi-En Tsai, Hunter N. Ratliff, Norihiro Matsuda, Hiroshi Iwase, Nobuhiro Shigyo, Lembit Sihver and Koji Niita. , J. Nucl. Sci. Technol. 55, 684-690 (2018).

Taprogge, 2021: Adjustment of the iodine ICRP population pharmacokinetic model for the use in thyroid cancer patients after thyroidectomy. Taprogge J, Carnegie-Peake L, Murray I, Gear JI, Flux GD. Radiol Prot. 2021 Nov 11;41(4)